

Article access online



 OPEN ACCESS

Received: 02.09.2024

Accepted: 18.11.2024

Published: 12.12.2024

Citation: Goel V, Roy A, Maiti N. (2024). 3-D Electromagnetic Simulations for Electron Beam Positioning. International Journal of Electronics and Computer Applications. 1(2): 45-49. <https://doi.org/10.54839/ijeaca.v1i2.6>

* **Corresponding author.**

vanyagoel2012@gmail.com

Funding: None

Competing Interests: None

Copyright: © 2024 Goel et al. This is an open access article distributed under the terms of the Creative Commons Attribution License, which permits unrestricted use, distribution, and reproduction in any medium, provided the original author and source are credited.

ISSN

Print: XXXX-XXXX

Electronic: 3048-8257

3-D Electromagnetic Simulations for Electron Beam Positioning

Vanya Goel^{1*}, Amitava Roy², Namita Maiti³

¹ Assistant Professor, KIET Group of Institutions, Delhi-NCR, India

² Scientific Officer-G, Homi Bhabha National Institute, Bhabha Atomic Research Centre, Mumbai, Maharashtra, India

³ Retd. Scientific Officer-H, Homi Bhabha National Institute, Bhabha Atomic Research Centre, Mumbai, Maharashtra, India

Abstract

In this paper, 3-D simulations have been carried out to position electron beam of high-power (60 kW, 60 kV, 1 A) linear electron gun. These simulations are highly significant for indirectly heated electron guns due to the presence of an additional electrode. In the inter-electrode space, particle trajectories, effective electron beam cross-section bombardment at solid cathode and electron beam emittance are crucial beam characteristics. Detailed 3-D electrostatic, electromagnetic and particle tracking simulations in inter-electrode region as well as in post-anode region have been successfully done for two parametric variations of electron gun. These include 1) Filament-solid cathode interspacing: Interelectrode region and 2) Magnetic coil current and corresponding magnetic field: Post-anode region. CST Studio Particle Tracking Module simulation software has been used, employing adaptive mesh refinement for fine meshing to ensure high accuracy results.

Keywords: Electron Gun; Electron beam; Optimization techniques; High voltage applications

Introduction

An electron gun is an electrical device which generates a focused electron beam that can be used for various applications such as material processing, laser-isotope separation, accelerator technology, etc. An electron gun fundamentally in construction can be of two types: Directly Heated and Indirectly Heated. This paper contributes to the stable operation of an Indirectly Heated Cathode-based Electron Gun (IHCEG). The filament is resistively heated through passage of direct current flow however, the

solid cathode is indirectly heated through electron bombardment⁽¹⁾. In the case of IHCEG, achieving stable operation upon application of high voltages is a serious concern. This is because, during high-power operation, the additional electrode i.e., solid cathode and associated inter-electrode region between filament and solid cathode becomes highly vulnerable to loss of electrons due to electron scattering, low emission electron density due to space charge effect, non-uniform electron distribution at solid cathode and low emission current density^(2,3). Thus, particle tracking in the inter-electrode region

between filament and solid cathode becomes very important for effective high-power IHCEG operation and device performance optimization⁽⁴⁾. In this paper, detailed 3-D modelling and particle tracking simulations have been carried out to study and analyze high voltage electron gun performance and beam positioning. The particle trajectory simulations are obtained in the presence of electrostatic as well as electromagnetic fields in order to achieve output electron beam with desired beam energy, beam focusing and beam bending. 3-D simulations have been done for geometric, electrical, and magnetic parameters of the IHCEG. The major parameters that determine beam trajectory shape and positioning in the inter-electrode and post-anode region are electric and magnetic fields respectively⁽⁵⁾. The electric field provides the necessary electrostatic focusing and beam shaping in the inter-electrode region. The magnetic field provides the required electromagnetic beam shaping and focusing in the post-anode region^(6,7). The region where the electron beam is meant to fall for desired application such as refractory metal melting, evaporation and coating, etc. is commonly known as target plane⁽⁸⁾. Electric field in the inter-electrode region is affected by the inter-electrode spacing and magnetic field in the post-anode region is mainly affected by the magnetic current i.e., Helmholtz coil current and the generated uniform magnetic field^(9,10). Through variation of these parameters, the electron beam cross-section, shape and emittance have been investigated in this paper.

3-D Simulation Model of IHCEG

Here, modelling and simulation of a high-power IHCEG has been done. Material properties of all the components of IHCEG have been taken into consideration while simulation in order to get practical experimental conditions. Modeling and design have been done by using CST Studio Particle Tracking Module⁽¹¹⁾. Detailed schematic diagram of IHCEG is shown in Figure 1(a). Different components of the electron gun have been illustrated in detail. Notably, Figure 1(a) shows the required 2700-bent electron beam that should fall at crucible or precisely at target plane and Figure 1(b) shows the target plane.

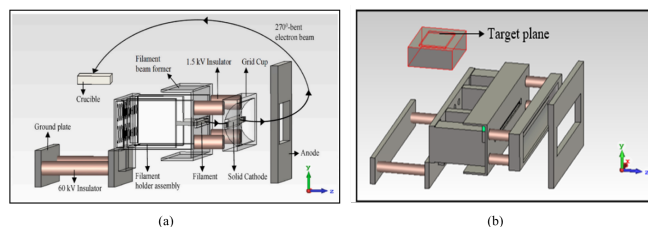


Fig 1. (a) Schematic diagram of IHCEG (b) Target plane

The design of IHCEG includes: 1) filament and solid cathode which act as electron emitters, 2) filament beam

former and grid cup which act as focusing electrodes, 3) HV insulators for electrical insulation and physical mechanical support⁽¹²⁾. In the output, a well-focussed electron beam is required which emerges from anode, bent by 2700 and falls at the target plane for further action^(13,14). Generally, in a transverse electron gun, crucible with target material is placed at 2700 with respect to electron gun so as to prevent metallic coating on gun components due to evaporation of target material^(15,16). In the subsequent section, 3-D simulations have been performed in order to obtain and analyse 2700-bent electron beam at the crucible or more specifically at target plane for desired application.

3-D Simulations For Electron Beam Positioning

In order to carry out the study and analysis of 3-D electron beam, geometric, electrical and magnetic simulation and modelling is done with the help of CST Studio Particle Tracking module. The electron gun is modelled with the physical parameters and dimensions as discussed in detail in⁽¹²⁾. Further, electrostatic simulations have been carried out after electron gun modelling and design in which appropriate electric potentials have been applied to the electron gun electrodes. The respective voltages applied to filament and solid cathode are as follows: filament and beam former at -61.5 kV floating potential. Solid cathode and grid cup at -60 kV floating potential. The anode and crucible grounded. In electromagnetic simulations, electric fields are produced by applying electric potentials and uniform magnetic field is produced by using pair of Helmholtz coils. In⁽¹²⁾, optimum value of magnetic current was found out to be 75 mA, providing a bending beam radius of 198 mm. In 3-D particle tracking simulations, 3-D particle trajectories are computed by evaluating the electromagnetic fields. Detailed information regarding electron beam in the entire computational domain has been obtained such as individual trajectory's 3-D location/coordinates (x, y, and z), electron energy levels (eV) at various time instances right from point of beam emergence until beam reaches target plane such that better electron beam visualization and analysis in 3-D plane can be performed^(17,18). For characterization and positioning of electron beam obtained from the indirectly heated cathode-based electron gun, two parametric variations of electron gun have been considered and simulated:

Filament-Solid Cathode Interspacing: Inter-electrode region

Electron beam characterization has been performed by investigating the electron beam size and emittance at ten different filament-solid cathode interspacing. "d" is considered as the inter-spacing distance from 1 mm to 10 mm in interval of 1

mm. For these different interspacing, the gun iterations have been performed. For ensuring high accuracy of results, adaptive mesh refinement was employed. The schematic diagram showing the arrangement of filament and solid cathode for different “d” is as shown in Figure 2. The filament has an emitting cross-section of $110 \times 3 \text{ mm}^2$ and that of solid cathode is $110 \times 4.5 \text{ mm}^2$. Electron beam diameter and emittance at the backside of solid cathode have been evaluated by using particle monitors. 3-D simulation result of electron beam trajectories in between filament and solid cathode for $d = 1, 5$ and 10 are shown in Figure 3 (a), (b) and (c) respectively.

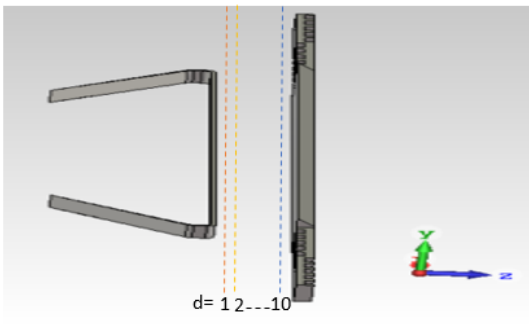


Fig 2. Arrangement of filament and solid cathode showing different interspacing (not to scale)

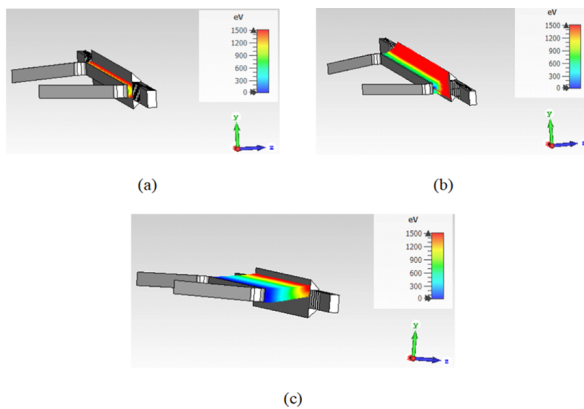


Fig 3. 3-D simulation result of electron beam trajectories in between filament and solid cathode (a) $d=1$ (b) $d=5$ (c) $d=10$

Electron beam cross-section at backside of solid cathode for $d = 1, 5$ and 10 are shown in Figure 4(a), (b) and (c) respectively. Table 1 shows numerical values from electron gun simulation data for beam cross-section and emittance.

From Table 1, it is seen that for $d < 5 \text{ mm}$, at the backside of solid cathode electron beam cross-section is less. This is because due to less interspacing between solid cathode and filament, electrons majorly concentrate fall at the center of solid cathode and does not cover it completely as can be seen in Figure 3(a). At higher interspacing i.e., $d > 5 \text{ mm}$, as the

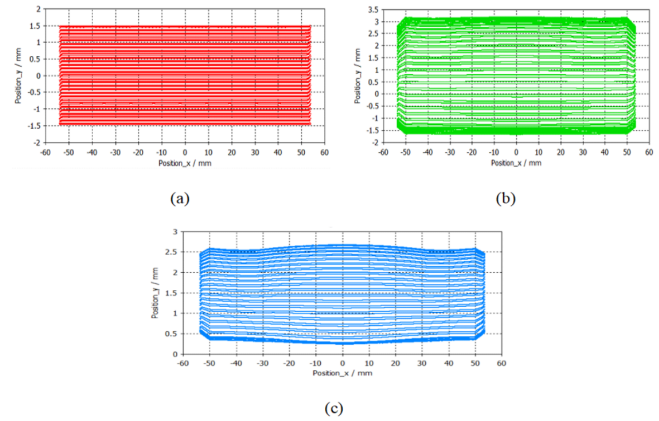


Fig 4. Electron beam cross-section at solid cathode backside for (a) $d=1$ (b) $d=5$ (c) $d=10$

Table 1. Electron Beam Cross-Section and Beam Emittance For $d = 1$ to 10

S.No	Filament-Solid Cathode Spacing “d” (mm)	Electron beam cross-section at backside of solid cathode (mm^2)	Electron beam emittance (mm-rad)	
			x	y
1	1	108 x 3	0.042	0.012
2	2	108.5 x 3.15	0.162	0.064
3	3	109 x 3.55	0.245	0.089
4	4	109.2 x 4	0.255	0.117
5	5	109.8 x 4.45	0.275	0.451
6	6	110 x 4.1	0.288	0.33
7	7	110 x 3.85	0.304	0.29
8	8	110 x 3.1	0.317	0.23
9	9	110 x 2.35	0.339	0.215
10	10	110 x 2.15	0.374	0.16

electron beam bends under the influence of magnetic field hence, portion of beam falling at the solid cathode backside is less, this can be seen in Figure 3 (c). However, for $d = 5 \text{ mm}$, it was found out that the electron beam cross-section at backside of solid cathode was maximum. This was found out to be the optimum interspacing between filament and solid cathode as the electron beam emitted from filament covers entirely the solid cathode backside leading to uniform electron bombardment, as can be seen in Figure 3 (b).

Magnetic coil current and magnetic field: Post-anode region

In the IHCEG setup illustrated in this paper, Helmholtz coils have been used to provide the required uniform magnetic field for beam deflection and focusing at target plane. A schematic diagram showing IHCEG setup along with Helmholtz coils is shown in Figure 5.

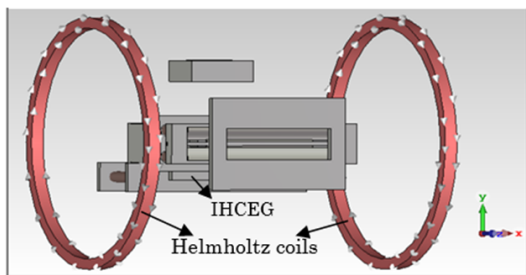


Fig 5. IHCEG setup along with Helmholtz coils

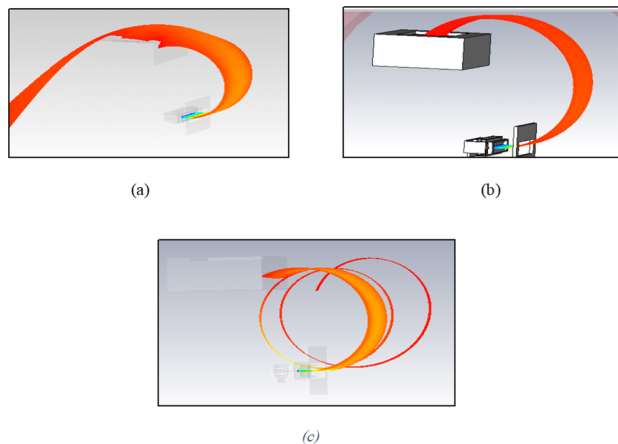


Fig 6. Simulation result of electron beam at Helmholtz coil current of (a) 25 mA (b) 75 mA (c) 125 mA

Table 2. Electron Beam Cross-Section and Beam Emittance at Different Magnetic Coil Currents

S.No.	Helmholtz coil current (mA)	Electron beam radius (mm)	Electron beam cross-section at target plane (mm ²)	Electron beam emittance (mm-rad)	
				x	z
1	25	310	150.8x19.6	0.789	0.386
2	50	260	138.4x18.2	0.628	0.375
3	75	198	76 x 16.5	0.310	0.481
4	100	148	128.5x17.6	0.569	0.566
5	125	100	138.7x18.3	0.797	0.628

Helmholtz coils is a pair of magnetic coils having equal number of turns, carrying current in the same direction, and placed co-axially with interspacing equal to coil diameter^(19,20). These coils provide uniform magnetic field in the region between the coils. Thus, the electron beam generated by the electron gun can be effectively deflected and focused

towards the target plane by providing appropriate magnetic field. To achieve this, 3-D electromagnetic simulations have been carried out such that the coil current was varied and the electron beam bending radius was monitored. The simulations were performed at optimum filament-solid cathode and solid cathode-anode interspacing of 5 mm and 15 mm respectively. For different coil currents, the electron beam trajectory is traced, and electron beam cross-section and emittance have been recorded. 3-D simulation result of electron beam trajectories at Helmholtz coil current of 25 mA, 75 mA and 125 mA are shown in Figure 6(a), (b) and (c) respectively. It was observed that for coil current less than 75 mA, electron beam radius was greater than crucible dimensions and hence, electron beam trajectories tend to fall beyond the crucible as well as target plane. For coil current more than 75 mA, electron beam radius was smaller than crucible dimensions and hence, electron beam trajectories tend to fall below the crucible as well as target plane.

However, at 75 mA, electron beam was found to be falling at the centre of target plane with a bending radius of 198 mm. Also, a well-focused electron beam was obtained with a smaller cross-section as well as lower beam emittance. The numerical values of obtained electron beam bending radius, cross-section at target plane (length along x-axis and width along z-axis) and beam emittance at different Helmholtz coil currents has been tabulated in Table 2. Minimum electron beam cross-section and beam emittance was obtained at Helmholtz coil current of 75 mA.

Conclusion

The work presented in this paper includes positioning of electron beam of an IHCEG. The work includes 3-D simulations for measurement of beam cross-section and beam emittance in the region between filament and solid cathode, between solid cathode and grid cup and at target plane in the post-anode region. Parametric variation of inter-electrode spacing between filament and solid cathode have been investigated. For desired beam positioning in the post-anode region, magnetic parameters including Helmholtz coil current, and the corresponding magnetic field has been varied and analysed with respect to beam positioning. It was found out that for 5 mm filament-solid cathode interspacing, beam cross-section at backside of solid cathode was maximum. Most uniform electron beam distribution at solid cathode backside was obtained from a strip shaped filament. By applying Helmholtz coil current of 75 mA, a well-focused electron beam appropriately falling at center of target plane was obtained.

References

- 1) Schiller S, Heisig U, Panzer S. Electron Beam Technology. New York. John Wiley & Sons. 1982. Available from: https://books.google.co.in/books/about/Electron_Beam_Technology.html?id=QRJTAAAMAAJ&redir_esc=y.
- 2) Maiti N, Bade A, Tembhare GU, Patil D, Dasgupta K. Design and development of improved indirectly heated cathode based strip electron gun. *Review of Scientific Instruments*. 2015;86(2). Available from: <https://doi.org/10.1063/1.4909535>.
- 3) Abramyan EA, Ligachev AE. Applications of intense electron beam for the processing of materials. *International Journal of Radiation Applications and Instrumentation Part C Radiation Physics and Chemistry*. 1988;31(4-6):829–841. Available from: [https://doi.org/10.1016/1359-0197\(88\)90265-2](https://doi.org/10.1016/1359-0197(88)90265-2).
- 4) David J, Ives R, Tran H, Bui T, Read ME. Computer Optimized Design of Electron Guns. *IEEE Transactions on Plasma Science*. 2008;36(1):156–168. Available from: <https://doi.org/10.1109/TPS.2007.913884>.
- 5) Lewis BM, Tran HT, Read ME, Ives RL. Design of an Electron Gun Using Computer Optimization. *IEEE Transactions on Plasma Science*. 2004;32(3):1242–1250. Available from: <https://doi.org/10.1109/TPS.2004.827572>.
- 6) Palacios-Serrano G, Hannon F, Hernandez-Garcia C, Poelker M, Baumgart H. Electrostatic design and conditioning of a triple point junction shield for a -200 kV DC high voltage photogun. *Review of Scientific Instruments*. 2018;89(10). Available from: <https://doi.org/10.1063/1.5048700>.
- 7) Nishimori N, Nagai R, Matsuba S, Hajima R, Yamamoto M, Honda Y, et al. Experimental investigation of an optimum configuration for a high-voltage photoemission gun for operation at ≥ 500 kV. *Physical Review Accelerators and Beams*. 2014;17(5):1–17. Available from: <https://doi.org/10.1103/PhysRevSTAB.17.053401>.
- 8) Wang P, Dong Q, Wu G, Liu J, Li W. Practical design of triple junction for a 90 kV electron gun. *IEEE Transactions on Dielectrics and Electrical Insulation*. 2019;26(4):1043–1047. Available from: <https://doi.org/10.1109/TDEI.2019.007818>.
- 9) Gallagher HE. The Design and Performance of Grid-Controlled High Perveance Electron Guns. *IRE Transactions on Electron Devices*. 1959;6(4):390–396. Available from: <https://doi.org/10.1109/T-ED.1959.14569>.
- 10) Pierce JR. Theory and design of electron beams. New York, N. Y.: D. Van Nostrand Co., Inc. 1954.
- 11) CST STUDIO SUITE-Charged Particle Simulation. 2020. Available from: <https://space.mit.edu/RADIO/Documentation/CST%20Studio%20Suite%20-%20Charged%20Particle%20Simulation.pdf>.
- 12) Goel V, Roy A, Maiti N. Performance optimization of indirectly heated cathode based electron gun by controlling high voltage surface flashover and beam positioning at target plane. *Vacuum*. 2022;196. Available from: <https://doi.org/10.1016/j.vacuum.2021.110759>.
- 13) Goel V, Roy A, Maiti N. Improvement of Electron Gun Breakdown Performance through Surface Flashover and Discharge Studies. *IEEE Transactions on Electron Devices*. 2023;70(7):3833–3841. Available from: <https://doi.org/10.1109/TED.2023.3273513>.
- 14) Dikshit B, Bhatia MS. A Novel 2700 Bent-Axial-Type Electron Gun and Positioning of its Electron Beam Spot on the Target. *IEEE Transactions on Electron Devices*. 2010;57(4):939–945. Available from: <https://doi.org/10.1109/TED.2010.2040663>.
- 15) Majumdar A, Sahu GK, Thakur KB, Mago VK. Electron-beam generated copper plasma: formation and cross-field propagation. *Journal of Physics D: Applied Physics*. 2010;43(7). Available from: <https://iopscience.iop.org/article/10.1088/0022-3727/43/7/075204>.
- 16) Goel V, Roy A, Maiti N. 3-D Analysis of Electron Beam Shape at Target Plane through Parametric Variation of an Indirectly Heated Cathode-based Electron Gun. In: 14th International Conference on Electron Beam Technologies (EBT 2022), vol. 2443 of Journal of Physics: Conference Series. IOP Publishing. 2023;p. 1–7. Available from: <https://iopscience.iop.org/article/10.1088/1742-6596/2443/1/012018>.
- 17) Goel V, Roy A, Maiti N. A Novel Technique for Optimizing 270°-Bent Electron Gun for Evaporation Applications. *IEEE Transactions on Plasma Science*. 2020;48(9):3098–3108. Available from: <https://doi.org/10.1109/TPS.2020.3018415>.
- 18) El-Saftawy AA, Elfalaky A, Ragheb MS, Zakhary SG. Investigation of Beam Performance Parameters in a Pierce-Type Electron Gun. *Science and Technology*. 2012;2(6):191–197. Available from: <https://doi.org/10.5923/j.scit.20120206.08>.
- 19) Bernius MT, Man KF, Chutjian A. An electrostatically and a magnetically confined electron gun lens system. *Review of Scientific Instruments*. 1988;59:2418–2423. Available from: <https://doi.org/10.1063/1.1139920>.
- 20) Masood K, Bhatti SA, Rafiq M. Magnetically confined high power thermionic line source emitter assembly. *Vacuum*. 2005;77(2):101–110. Available from: <https://doi.org/10.1016/j.vacuum.2004.08.005>.